Molecular Therapy
Original Article

DDX5 mRNA-targeting antisense oligonucleotide as a new promising therapeutic in combating castration-resistant prostate cancer

Thi Khanh Le,[1,2] Chaïma Cherif,[1] Kenneth Omabe,[1] Clément Paris,[1] François Lannes,[1,5] Stéphane Audebert,[3] Emilie Baudelet,[3] Mourad Hamimed,[4] Dominique Barbolosi,[4] Pascal Finetti,[1] Cyrille Bastide,[5] Ladan Fazli,[6] Martin Gleave,[6] François Bertucci,[1] David Taïeb,[1,7,8] and Palma Rocchi[1,8]

[1]Predictive Oncology Laboratory, Centre de Recherche en Cancérologie de Marseille, Inserm UMR 1068, CNRS UMR 7258, Institut Paoli-Calmettes, Aix-Marseille University, 27 Bd. Leï Roure, 13273 Marseille, France; [2]Department of Life Science, University of Science and Technology of Hanoi, Hanoi 000084, Vietnam; [3]Marseille Protéomique, Centre de Recherche en Cancérologie de Marseille, INSERM, CNRS, Institut Paoli-Calmettes, Aix-Marseille University, 13009 Marseille, France; [4]Inria – Inserm team COMPO, COMPutational pharmacology and clinical Oncology, Centre Inria Sophia Antipolis – Méditerranée, Centre de Recherches en Cancérologie de Marseille, Inserm U1068, CNRS UMR7258, Institut Paoli-Calmettes, Aix-Marseille University, 27 Boulevard Jean Moulin, 13005 Marseille, France; [5]Urology Deparment, AP-HM Hospital Nord, Aix-Marseille University, 13915 Marseille Cedex 20, France; [6]The Vancouver Prostate Centre, University of British Columbia, Vancouver, BC V6H 3Z6, Canada; [7]La Timone University Hospital, Aix-Marseille University, 13005 Marseille, France; [8]European Center for Research in Medical Imaging, Aix-Marseille University, 13005 Marseille, France

The heat shock protein 27 (Hsp27) has emerged as a principal factor of the castration-resistant prostate cancer (CRPC) progression. Also, an antisense oligonucleotide (ASO) against Hsp27 (OGX-427 or apatorsen) has been assessed in different clinical trials. Here, we illustrate that Hsp27 highly regulates the expression of the human DEAD-box protein 5 (DDX5), and we define DDX5 as a novel therapeutic target for CRPC treatment. DDX5 overexpression is strongly correlated with aggressive tumor features, notably with CRPC. DDX5 downregulation using a specific ASO-based inhibitor that acts on DDX5 mRNAs inhibits cell proliferation in preclinical models, and it particularly restores the treatment sensitivity of CRPC. Interestingly, through the identification and analysis of DDX5 protein interaction networks, we have identified some specific functions of DDX5 in CRPC that could contribute actively to tumor progression and therapeutic resistance. We first present the interactions of DDX5 and the Ku70/80 heterodimer and the transcription factor IIH, thereby uncovering DDX5 roles in different DNA repair pathways. Collectively, our study highlights critical functions of DDX5 contributing to CRPC progression and provides preclinical proof of concept that a combination of ASO-directed DDX5 inhibition with a DNA damage-inducing therapy can serve as a highly potential novel strategy to treat CRPC.

INTRODUCTION

Prostate cancer (PC) is the second most frequent cancer and the fifth most common cause of cancer deaths in men.[1] Most patients with advanced PC are treated with standard androgen deprivation therapy (ADT). Despite the initial response to ADT, patients tend to suffer from disease evolution to a castration-resistant state (CRPC) with pejorative outcomes.[2] The heat shock protein 27 (Hsp27) was found upregulated in the vast majority of CRPC cases and mediates tumor growth and drug resistance. Hsp27 inhibition by antisense oligonucleotide (ASO) and small interference RNA (siRNA) has been revealed to significantly restore tumor sensitivity to castration and chemotherapy in preclinical models.[3–5] We previously illustrated that Hsp27 stabilizes its critical oncogenic interacting proteins such as eukaryotic translation initiation factor 4 E (eIF4E), translationally controlled tumor protein (TCTP), and menin through its chaperon activites.[6–8] To get insight into the network of proteins or cellular functions that are regulated by Hsp27, a large-scale proteomic analysis was performed in our laboratory, and it suggested that DDX5 is an Hsp27-mediated protein in PC.[8] In addition, the established Hsp27 interactions identified DDX5 as a potential novel Hsp27-interacting protein in PC cells but not in the nonmalignant prostatic cells (T.K.L., unpublished data). DDX5 acts as an oncoprotein in a wide range of cancers and links to drug response in many studies.[9,10] Together, these observations led us to hypothesize that Hsp27 could confer CRPC emergence through DDX5, so DDX5 could serve as a high-potential therapeutic target for CRPC treatment.

DDX5, a member of the DEAD-box RNA helicase family, plays central roles in gene expression via participating in cellular RNA metabolism

Received 3 December 2021; accepted 9 August 2022;
https://doi.org/10.1016/j.ymthe.2022.08.005.

Correspondence: Palma Rocchi, Predictive Oncology Laboratory, Centre de Recherche en Cancérologie de Marseille, Inserm UMR 1068, CNRS UMR 7258, Institut Paoli-Calmettes, Aix-Marseille University, 27 Bd. Leï Roure, 13273 Marseille, France.
E-mail: palma.rocchi@inserm.fr

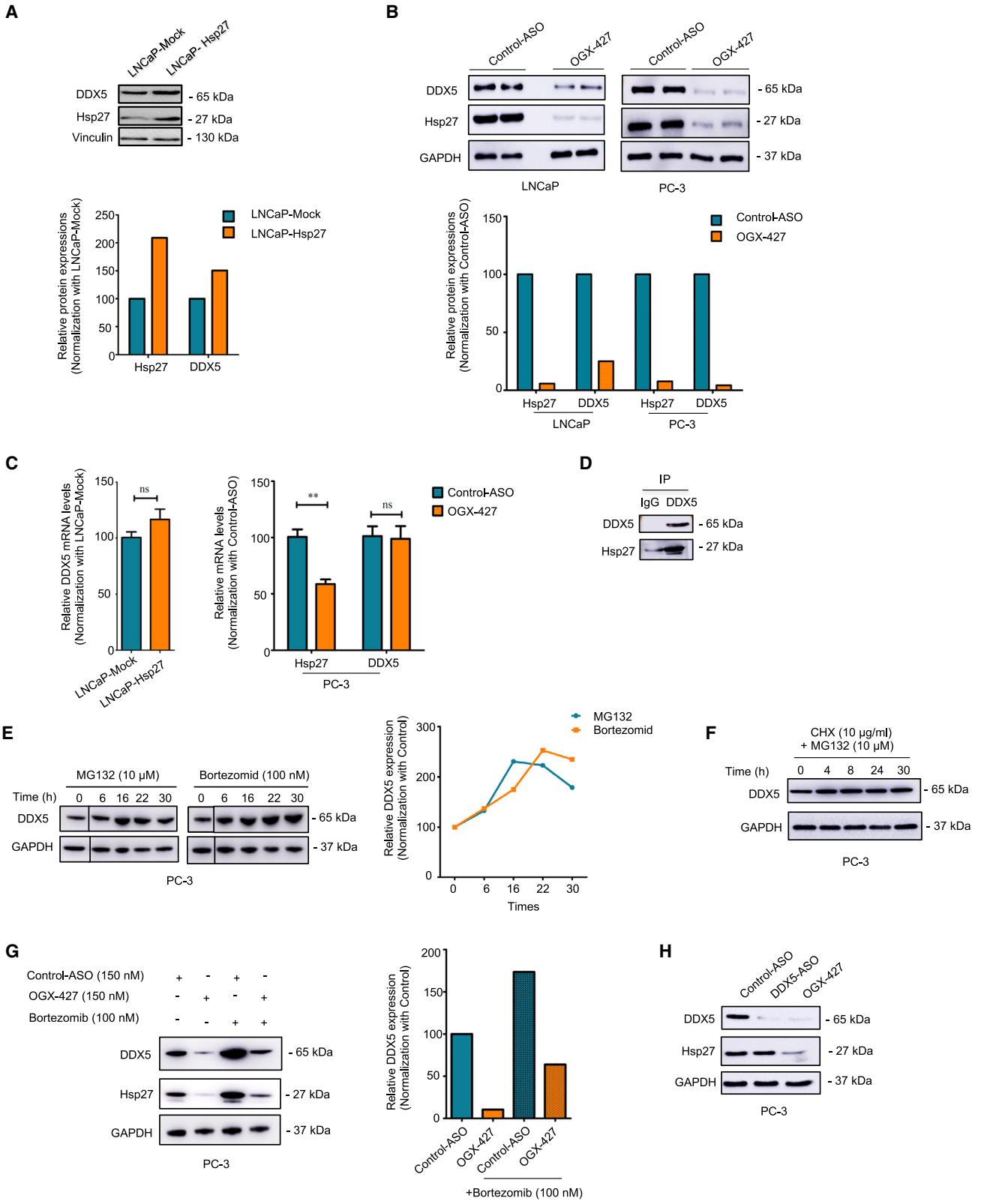

(legend on next page)

such as mRNA decay, ribosome biogenesis, splicing, and transcription.[11,12] DDX5 functions as a transcriptional co-activator for a number of highly regulated transcription factors, including estrogen receptor α,[13] β-catenin,[14] androgen receptor (AR),[15] and p53.[16] DDX5 is overexpressed in nearly 93% of human cancers[10] such as breast cancer[17] and PC.[18] In addition, DDX5 has been demonstrated to enhance cell proliferation, metastasis, and resistance to drugs through stimulating different oncogenic signaling mechanisms.[9,10]

In PC, DDX5 acts as an AR co-activator of transcription.[15] DDX5 interacts with β-catenin, a transcriptional co-regulator of activity; remarkably DDX5 was shown to promote cell survival and growth in AR-negative PC cell lines (DU-145, PC-3) by promoting mTORC1 signaling.[19] The oncogenic lncRNA CCAT1 was demonstrated to activate AR-mediated genes through interacting with DDX5, thereby promoting PC cell proliferation.[20] The previous study reported that DDX5 overexpression is linked to PC[18]; however, whether DDX5 expression level is upregulated in CRPC remains undefined.

This work aims to further characterize the oncogenic roles of DDX5 in PC, providing perspectives of ASO-directed DDX5 silencing in CRPC treatment. We show that Hsp27 positively regulates DDX5 protein levels, which in turn are associated with tumor growth and progression. The tissue microarray analysis (TMA) implies that DDX5 is a novel therapeutic target for CRPC remedy due to a strong positive correlation between DDX5 overexpression and CRPC. An ASO selectively targeting DDX5 mRNAs (DDX5-ASO, WO2021099394A1, 2021) is developed and illustrated in its high efficiency in the downregulation of DDX5 expression and cell proliferation both *in vitro* and *in vivo*. In addition, we determine and analyze DDX5 protein interactions using four human prostate cell lines (PNT1A, LNCaP, DU-145, and PC-3) recapitulating different disease stages. Compared with the normal prostate cell (NM) and castration-sensitive (CS) cells, the DDX5 interaction proteins in the castration-resistant (CR) cells are exclusively enriched in functions mainly related to DNA damage response, transcription regulation, RNA stability, and DNA conformation changes, which could promote tumor progression and therapeutic resistance in PC. Interestingly, we identify a new critical role of DDX5 in DNA damage repair in CRPC, and we demonstrate that DDX5 inhibition via DDX5-ASO enhances treatment sensitivity, which opens new therapeutic perspectives for PC patients.

RESULTS

Hsp27 highly regulates DDX5 expression via preventing DDX5 protein from proteasomal degradation

Our recent works based on proteomic approaches have suggested that DDX5 is a Hsp27-regulated protein[8] and probably interacts with Hsp27 in PC cells (T.K.L., unpublished data). Here, we confirmed that the DDX5 protein level is higher in the LNCaP-Hsp27 than in LNCaP-mock cells (Figure 1A). Hsp27 depletion by OGX-427 results in remarkable decreases of DDX5 levels in both LNCaP and PC-3 cell lines (Figure 1B). However, DDX5 mRNA expression is not altered under both conditions of Hsp27 upregulation and downregulation (Figure 1C), implying that Hsp27 does not regulate DDX5 expression either at transcriptional level or through controlling DDX5 mRNAs stability.

On the other hand, the interaction between Hsp27 and DDX5 is verified by western blot following immunoprecipitation (IP) in PC-3 cells (Figure 1D). Since the ubiquitin-proteasome system was previously reported to mediate DDX5 degradation,[21,22] we examined whether DDX5 protein stability is regulated by the 26 S proteasome in PC. The CR PC-3 cells were treated with either MG132 or bortezomib (proteasome inhibitors) with or without cycloheximide (CHX, an inhibitor of *de novo* protein synthesis). DDX5 levels increased in the presence of the proteasome inhibitors (Figure 1E); meanwhile, they were stable by the combination of both MG132 and CHX (Figure 1F). These results indicate that DDX5 degradation is mainly modulated by the proteasomal machinery in PC. Furthermore, adding bortezomib reverses the downregulation effect of OGX-427 on DDX5 protein levels (Figure 1G), suggesting that binding of Hsp27 to DDX5 can protect DDX5 protein from degradation by the proteasome.

To evaluate whether both proteins have mutual effects, we evaluated the Hsp27 protein expression upon DDX5 silencing. Hsp27 protein level was not changed due to DDX5 inhibition (Figure 1H). Therefore, Hsp27 controls DDX5 expression, and DDX5 does not regulate Hsp27 expression.

Figure 1. Hsp27 positively regulates DDX5 expression through preventing DDX5 protein from proteasomal degradation

(A) Western blotting (WB) analyzing the protein expression levels of DDX5 and Hsp27 in LNCaP-mock versus LNCaP-Hsp27 (overexpressed Hsp27) shows that DDX5 expression is higher in LNCaP-Hsp27 compared with the LNCaP-mock. (B) WB analyzing the protein expressions of DDX5 in the LNCaP and PC-3 cells transfected with OGX-427 (an Hsp27-targeting ASO) or control-ASO reveals that DDX5 protein expression decreased dramatically upon Hsp27 depletion. (C) Hsp27 does not regulate DDX5 at transcriptional level. qRT-PCR analysis showed that DDX5 mRNA levels are similar in both LNCaP-mock and LNCaP-Hsp27 cells. The mRNA levels of both DDX5 and Hsp27 are evaluated by qRT-PCR analysis using the PC-3 cells transfected with OGX-427 or control-ASO. The DDX5 mRNA level is constant upon Hsp27 knockdown. Sample t test was performed to compare the relative mRNA levels between two samples: LNCaP-mock versus LNCaP-Hsp27, OGX-427 versus control-ASO-transfected PC-3 cells. $^{**}p < 0.01$; ns, non-significant. (D) Confirmation of the interaction between Hsp27 and DDX5. DDX5 IP followed by WB analysis showed that Hsp27 was present in the IP using anti-DDX5 antibody. (E and F) DDX5 stability is controlled by the proteasome pathway in PC. Proteasome inhibition using either 10 μM MG132 or 100 nM bortezomib induces accumulation of DDX5 protein at the indicated times (E). Proteasome inhibitor combined with an inhibitor of *de novo* protein synthesis, CHX (cycloheximide), conserves DDX5 protein levels (F). (G) Hsp27 prevents DDX5 from proteasome degradation. PC-3 cells were transfected with OGX-427 or control-ASO at 150 nM concentration for 2 days, followed by incubation with or without 100 nM bortezomib for 24 h. WB analysis shows that the proteasome inhibitor bortezomib can reverse the downregulation of DDX5 induced by OGX-427. (H) DDX5 does not control Hsp27 protein abundance. WB analyses of the DDX5 and Hsp27 expression upon either Hsp27 knockdown by OGX-427 or DDX5 downregulation by DDX5-ASO in PC-3 cells. Hsp27 protein expression is stable upon DDX5 depletion.

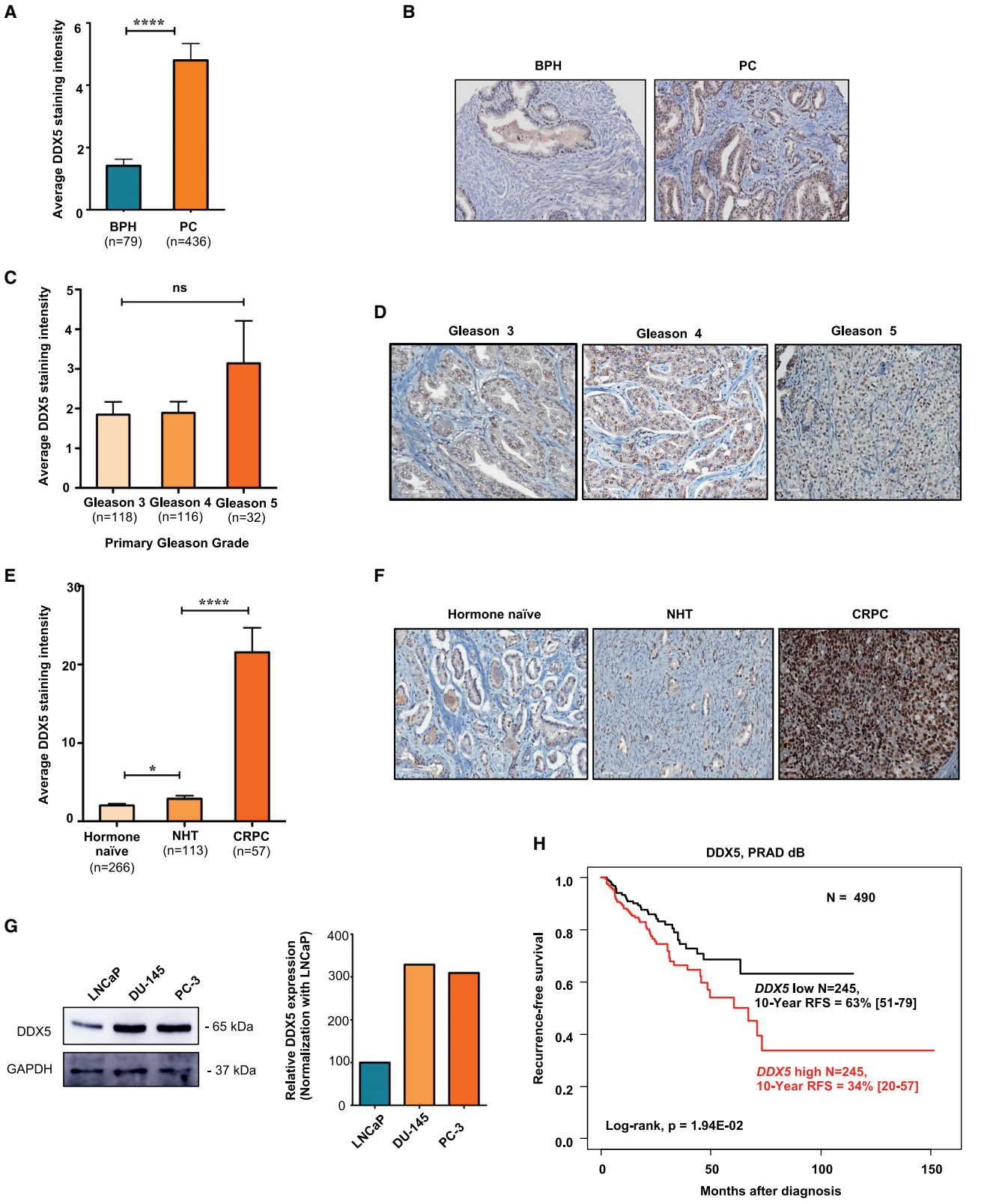

(legend on next page)

Elevated DDX5 protein expression is strongly associated with PC progression and castration-resistant phenotype

We examined DDX5 expression by immunohistochemistry (IHC) in a large tissue microarray series of different stages of PC specimens. As shown in Figures 2A and 2B, PC has a significantly higher level of DDX5 protein expression than benign prostatic hyperplasia (BPH). Although we found DDX5 upregulation in high Gleason scores, no statistical significance was observed, certainly due to tumor heterogeneity and the small number of samples in the Gleason 5 group (n = 32). Among the 266 PC specimens analyzed, Gleason grade 5 PC has the strongest DDX5 expression, followed by Gleason grades 4 and 3 (Figures 2C and 2D). Of note, DDX5 expression is remarkably upregulated in CRPC, with an average DDX5 staining intensity that is 10.56 times and 7.3 times higher than in hormone naive and neoadjuvant hormonal therapy (NHT) tumors, respectively (Figures 2E and 2F). This is in an agreement with DDX5 overexpression observed in CR cell lines (DU-145 and PC-3) compared with the CS LNCaP cell line (Figure 2G). The DDX5 subcellular localization was persistent across all the specimens. Furthermore, high expression levels of DDX5 mRNA positively correlated with poor recurrence-free survival (RFS), where 10-year RFS values of group "DDX5 high" and "DDX5 low" are 34% and 63%, respectively ($p = 1.94 \times 10^{-2}$, Figure 2H). Taken together, these results indicate that DDX5 could represent a novel potential target for CRPC treatment.

ASO-directed DDX5 silencing significantly decreases CRPC proliferation in both *in vitro* and *in vivo* models

To specifically inhibit DDX5 expression, we first designed 93 ASOs potentially acting on the human DDX5 mRNA sequence (hASO) (Table S1 and Figure S1). The first screening that tested 13 hASOs showed that hASO51 effectively inhibits DDX5 expression (Figure 3A). Subsequently, the screening of DDX5-ASOs was continued to find out a bispecific sequence of both human and murine forms (hmASOs), allowing us to identify potential toxic effects of DDX5 inhibition in xenografted mice. We tested eight bispecific sequences distributed uniformly over the entire target sequence at different locations of the mRNA in addition to hASO51. The hmASO3 is shown to effectively downregulate DDX5 protein expression (Figure 3B) and in a dose-dependent manner like hASO51 (Figure 3C). Moreover, DDX5 inhibition induced by both hASO51 and hmASO3 results in significant decreases of cell viability in CR PC-3 (Figure 3D) and in two LNCaP-derived cell lines (Figure S2).

Subsequently, we assessed the effect of DDX5 downregulation via DDX5-ASO (hmASO3) on the development of PC-3 xenograft tumors. The mice group treated with DDX5-ASO had a significant delay in tumor growth compared with the group treated with control-ASO (***$p < 0.001$, using repeated measures ANOVA) (Figures 3E and S3; Table S2). Furthermore, the population pharmacodynamic modeling approach was used to characterize the tumor growth kinetics and to quantify the effect of the ASO treatment on tumor size evolution.[23] The Gompertz model was selected as it can reflect the sigmoidal nature of growth and fit to the observed data significantly better than other models (Figure 3F, left and middle panels, and supplemental information). The inclusion of the treatment groups in the model produced a statistically significant drop in the objective function ($\Delta OFV = 11$, p value for likelihood ratio test <0.001), demonstrating that tumor growth was inhibited significantly in the DDX5-ASO treatment group compared with the control group. Model predictions showed that individuals for whom the ASO treatment was administered showed a 20% decrease in maximum tumor volume (Figure 3F, right panel). During the experiment, the mice were healthy (supplemental information, Table S3) and reverse side effects regarding animal behaviors were not observed (data not shown).

The identified DDX5 protein interactions reveal a broad functional landscape of DDX5 in PC

To decipher how DDX5 could promote PC progression, we determined and analyzed protein interaction networks of the endogenous DDX5 in different human PC cells using immunoaffinity purification mass spectrometry (IP-MS). In total, 489 DDX5-associated proteins were identified, and we obtained 16, 44, 239, and 401 interaction candidates for PNT1A, LNCaP, DU-145, and PC-3, respectively (with the selection filter false discovery rate [FDR] of 0.01, so = 1; supplemental information, Table S4). Obviously, a correlation of the number of DDX5 binding proteins with the disease aggressiveness and CRPC was observed, suggesting that DDX5 may acquire more functions during PC progression. Of note, there are 48 candidates (12%) characterized as known DDX5 interactors in the published database (String.db), including very well-documented DDX5-interacting proteins such as TP53,[16] DHX9,[24] and CDK9[25] (Figure 4A). In addition, our identified interactome of DDX5 reinforces the interaction between DDX5 and Hsp27.

Classifying the DDX5-binding proteins based on the PANTHER 14.1 "molecular function" and "protein class" category shows that a majority of the DDX5 interactors are involved in binding to nucleic acid, and

Figure 2. DDX5 overexpression is associated with tumor progression and CRPC as clinically relevant

(A) DDX5 expression is significantly higher in prostate cancer (PC) compared with benign prostatic hyperplasia (BPH). (B) representative images of DDX5 staining show increased DDX5 expression in PC specimens compared with BPH. (C) results show a tendency for DDX5 expression to increase with increasing Gleason grade. (D) Representative images of DDX5 staining show increased staining intensity in Gleason grade 5 specimens. (E) The graph and the representative IHC images show that DDX5 expression is extremely higher in castration-resistant prostate cancer (CRPC) patients than in the hormone naive and neoadjuvant hormone therapy (NHT) tumors. (F) Representative images of DDX5 staining show a remarkable increase of DDX5 staining expression in CRPC specimens. (G) DDX5 is overexpressed in CR cells (DU-145 and PC-3) compared with CS cells (LNCaP). The DDX5 protein level was analyzed by western blot using total cell lysate from three different prostate cell lines (LNCaP, DU-145, and PC-3). DDX5 protein level was normalized with GAPDH, which was also used as loading control. Quantification illustrates that DDX5 expression levels in both CR lines are at about three times as high as in CS cells. (H) Kaplan-Meier RFS curves in the TCGA PRAD public samples. High expression level of DDX5 mRNAs is positively correlated with poor recurrence-free survival (RFS). According to the DDX5 mRNA levels, samples were classified into two groups, DDX5 high and DDX5 low, which have 10-year RFS rates of 34% and 63%, respectively in a pool of 490 informed patients. *$p < 0.05$; **$p < 0.01$; ***$p < 0.001$; ****$p < 0.0001$; ns, non-significant.

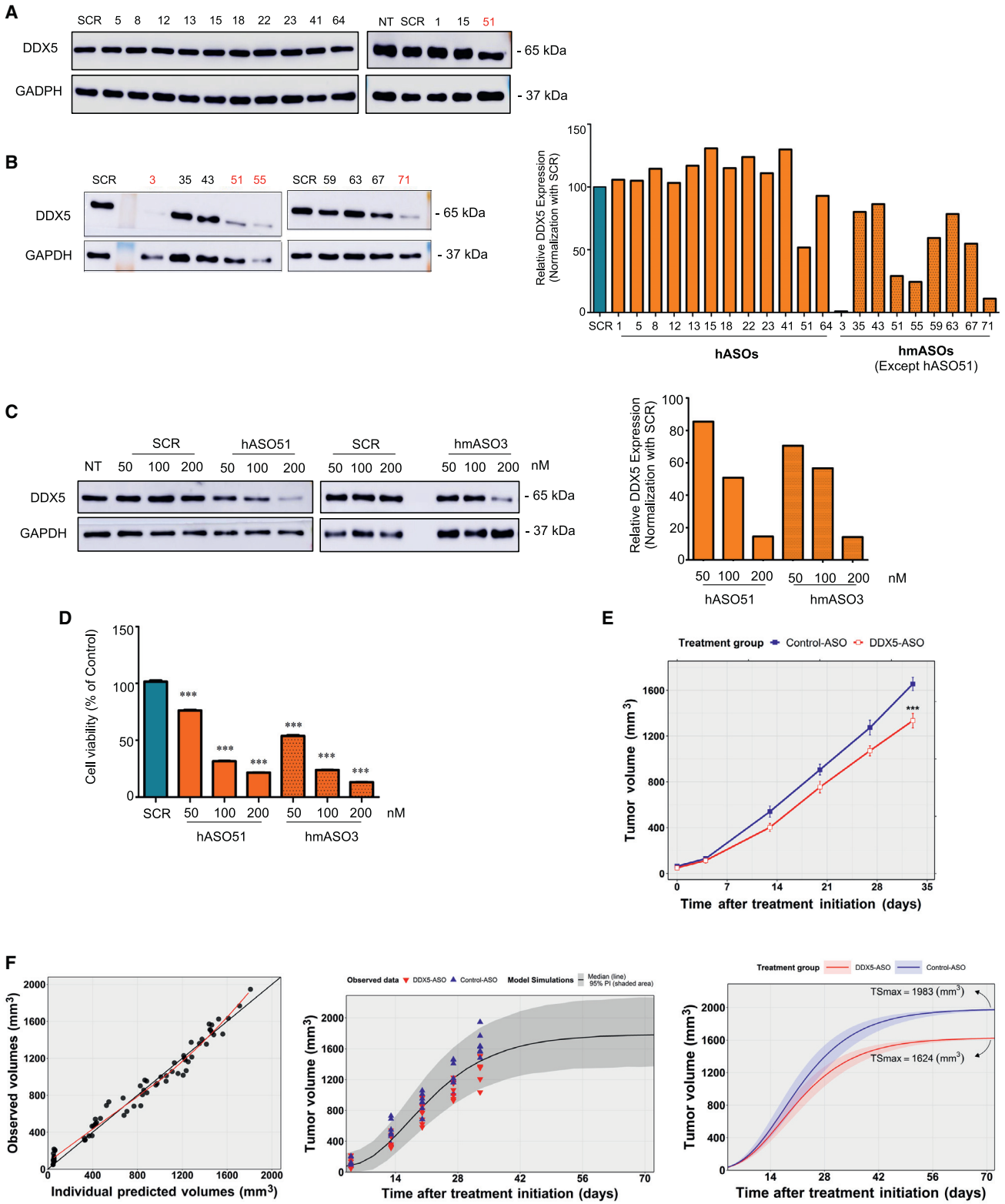

(legend on next page)

most of them are RNA-binding proteins (Figure S4). It also reveals several protein classes engaging with catalytic functions and illustrates a set of DDX5-associated proteins that act as transcription factors. According to gene ontology biological process (GO-BP) enrichment analysis, 126 and 79 biological functions are enriched with the significance levels of p = 0.05 and 0.005, respectively (Figure S5 and Table S4). As expected, a number of well-documented functions of DDX5 are observed (Figure 4B). Accordingly, we found that DDX5 plays a vital role in gene expression since a majority of DDX5 interactors (up to 57%) are engaged with this process (p = 0.0000E-100). DDX5 functions mainly in RNA processing ($p = 1.2751 \times 10^{-72}$), translation ($p = 1.8605 \times 10^{-71}$), ribosome biogenesis ($p = 1.8027 \times 10^{-42}$), and transcription ($p = 2.8988 \times 10^{-6}$). In addition, DDX5 modulates gene expression at posttranscriptional levels by regulating mRNA stability, RNA splicing, and translation. DDX5 is also found to participate in DNA topological change ($p = 1.2599 \times 10^{-8}$) and the cellular response to the DNA damage stimulus ($p = 4.4587 \times 10^{-3}$) including DNA repair ($p = 4.4272 \times 10^{-3}$).

By performing a functional enrichment analysis using Gprofiler with the CORUM 3.0 database for the identified DDX5-associated proteins, various enriched protein complexes corresponding to different functions are determined (Figure 4C). In agreement with GO-BP enrichment analysis, DDX5 was found to be tightly associated with the established protein complexes involved in ribosome biogenesis, protein synthesis in both cytoplasm and mitochondria, splicing, mRNA stability, transcription, and DNA repair (Table S5). In particular, DDX5 was found to be tightly associated with the IGF2BP2/IGF2BP3 complex (mRNA stability), toposome (cell cycle), the general transcription factor complex GTFIIH (transcription initiation and DNA repair), and 7SK RPN complex (transcription elongation) (Figure 4D).

Acquired biological functions of DDX5 in CR cells contribute to the switch from castration-sensitive PC to castration-resistant PC

Comparison of the enriched GOs obtained from DDX5 PPI networks in four cell lines using the ClusterProfiler R packages gives us clues about DDX5 functions promoting tumor progression and CRPC. Obviously, DDX5 was involved in many more biological functions in CR cells than in both CS and NM (Figure S6). Only three GO terms are common for both CS and CR cells, which are related to mRNA alternative splicing and mitochondrial translation. This implies that DDX5 could play a role in these two biological functions in both CSPC and CRPC. DDX5 could drive tumor progression and treatment resistance through its implications in DNA damage response, mRNA stabilization, transcription, and DNA conformation changes since these are the main cellular processes exclusively enriched in CRPC cells compared with CSPC (Figure 5A).

To verify several key interactions identified by MS analysis, IP followed by western blot analysis was carried out. Accordingly, DDX5 is confirmed to interact with the Ku70/Ku86 heterodimer (DNA repair, Figure 5B), NF45 (pri-ribosomal RNA processing, DNA repair, Figure 5B), GTF2H1 (transcription, DNA repair, Figure 5C), and YBX1 (mRNA stability, Figure 5D).

DDX5 inhibition with ASO technology restores treatment sensitivity in CR cells

A set of DDX5-binding proteins participating in DNA damage response was determined, and most of them are exclusively found in the CRPC cells and are implicated in two DNA repair pathways: non-homologous end joining (NHEJ) and nucleotide excision repair (NER) (Table 1). To decipher the role of DDX5 in the DNA repair, we examined the effect of DDX5 silencing on DNA repair recovery following radiations. The irradiation induced foci (IRIF) numbers (i.e., double-strand breaks) are higher in the DDX5-depleted cells compared with the control samples (DDX5 proficient cells) at 1, 7, and 24 h following irradiations (Figures 6A and 6B). In parallel with immunofluorescence, western blot analysis using both total and subcellular protein extracts illustrated that DDX5 knockdown decreases DNA repair efficiency (Figure 6C). Moreover, DDX5-ASO significantly enhances sensitivity to either irradiation or cisplatin compared with the control-ASO in CRPC DU-145 cells (Figures 6D and 6E). Particularly, combining DDX5-ASO with cisplatin can remarkably lower the GI_{50} of cisplatin up to nearly 3 times compared with the combination of control-ASO and cisplatin (3.838 versus 9.601 μM) (Figure 6E). Altogether, these imply that an overexpressed DDX5 could enhance DNA damage response and

Figure 3. ASO-directed DDX5 downregulation inhibits cell proliferation and PC-3 xenograft-tumor growth

(A–C) ASO screenings aim to define ASOs that inhibit DDX5 protein expression. Both hASO51 (human ASO) and hmASO3 (human/mouse) decrease DDX5 expression in a dose-dependent manner. (D) DDX5 knockdown by both hASO51 and hmASO3 significantly inhibits cell proliferation. The 3-(4,5-dimethylthiazol-2-yl)-2,5-diphenyl-2H-tetrazolium bromide (MTT) assay was done with biological triplication, and the data were analyzed using an independent sample t test. ***$p < 0.001$. (E) Mean (± SE) growth curve of PC-3 xenografted tumors (***$p < 0.001$, using repeated measures ANOVA). Male BALB/c nude mice harboring PC-3-derived xenografted tumor (7 mice/group) were daily intraperitoneally injected with 12.5 mg/kg control-ASO or DDX5-ASO (hmASO3) for 5 weeks. Tumor volume (mm^3) was measured weekly using a caliper in three perpendicular dimensions (X = width, Y = length, Z = depth) and calculated following the formula $X \times Y \times Z \times 0.5236$. The group treated with DDX5-ASO had a delay in tumor growth compared with the group of control-ASO. (F) Population pharmacodynamic modeling demonstrates that DDX5-ASO treatment significantly inhibits the tumor growth compared with the control group. The left and middle panels present the goodness of fit and predictive check (VPC) plot. Overall, these two plots indicate that the base model provided an acceptable fit to the observed data. Left panel: Individual predicted volumes versus observed volumes. Points represent individual predicted volumes plotted against observed volumes and are distributed evenly around the identity line, indicating that no major bias was observed across predicted values. Middle panel: Results of the scatter visual predictive check from 500 model-generated datasets. Solid triangles represent the observed volumes and are almost within the 95% prediction interval of the model, demonstrating that the model is able to reproduce the pharmacodynamic (PD) observations adequately. Right panel: Model prediction of tumor growth kinetics, depending on the received treatment, using the final model. Individuals for the mice treated with DDX5-ASO showed a 20% decrease in maximum tumor volume. SCR: scrambled oligonucleotide; NT: non- treated; TSmax, individual carrying capacity (predicted maximum tumor volume).

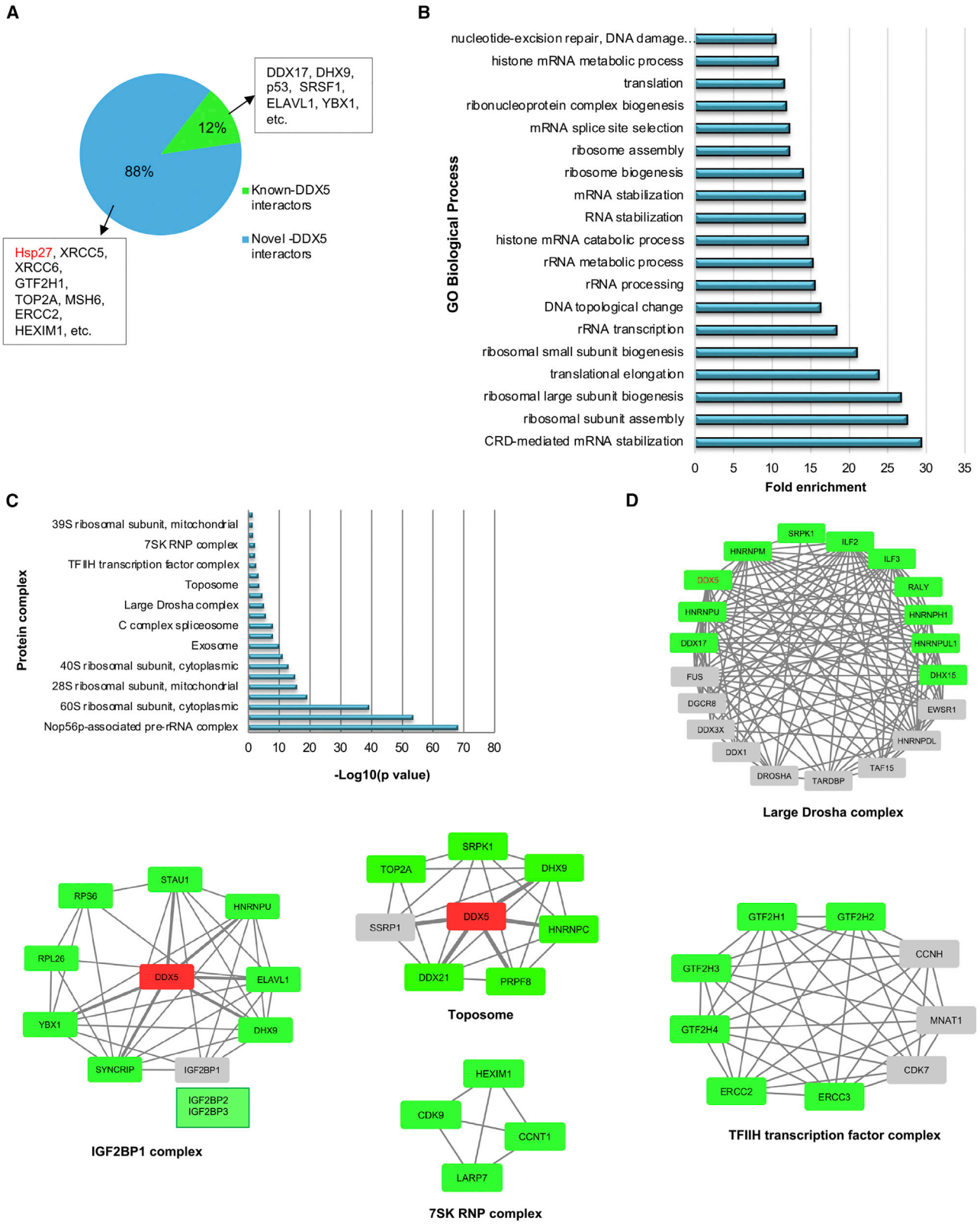

(legend on next page)

genome maintenance in CRPC, promoting tumor progression and treatment resistance (Figure 6F).

DISCUSSION

Nucleic acid (NA)-based technologies are currently developing rapidly with more than 15 NA drugs approved by the FDA and EMA and more than 2000 NA therapies undergoing clinical investigations.[26,27] Compared with siRNAs, ASO has several advantages such as its lower cost of production and easier synthesis and cell penetration without any transfecting agents.[28] Due to remarkable successes of mRNA-based vaccine during the current COVID-19 pandemic, mRNA targeting will represent a promising growing field in the next few years for personalized therapy in oncology. DDX5 has been identified as a cellular target of RX-5902[29] and resveratrol.[19] However, clinical translations of these agents have been hindered by certain limitations including lack of specificity. RX-5902 has not been tested in PC so far and probably does not work with AR-negative PC because the β-catenin/DDX5 interactions are AR dependent in PC.[15] As with many plant-based phytochemicals, the biggest challenge of resveratrol in clinical trials is its poor bioavailability once administered.[30] For these reasons, the DDX5 mRNA-directed ASO can serve as the most effective DDX5-targeting therapy for PC patients.

The obtained interaction maps of DDX5 in CR cells showed that DDX5 interacts with a number of critical oncogenic proteins linked to tumor progression and drug resistance in various malignancies such as IGF2BPs,[31] YBX1,[32,33] YY1,[34,35] and CTCF.[36] Most notably, we uncovered novel DDX5-interacting proteins involved in different DNA repair pathways in PC. DDX5 has been previously reported to engage in DNA damage response.[16] This was attributed via recruitment of both p53 and RNAPII to the p21 promoter upon irradiation stress, resulting in cell cycle arrest after DNA damage. DU-145 cells harbor p53 mutation, which was believed to produce non-functional protein, whereas the PC-3 is a null-TP53 cell line[37]; therefore, DDX5 might respond to the irradiation stimulated in a p53-independent manner in the PC-3 and DU-145 cells.

Emerging evidences highlight the central roles of DDX5 and other the RNA-interacting proteins in genome stability, notably in DNA repair.[38,39] R-loops or DNA-RNA hybrids are generated not only at active transcription sites by RNA polymerase but also around DNA break sites, and they play a fundamental function in DNA repair.[40] Aberrant R-loop formation can result in replication stress, DNA double-strand breaks, and genomic instability.[41,42] DDX5 associates with DNA:RNA hybrids,[43] unwinds unscheduled R-loops,[42] and DDX5 downregulation accumulates R-loop genome-wide, in chromosome regions with very high gene density and particularly at transcription start sites, transcription termination sites,[44] and at double-stranded breaks (DSBs).[45] Furthermore, DDX5 has been previously illustrated to promote DNA damage repair through acting as an active player in resolving R-loops near or at DSBs, thereby maintaining genomic stability.[41,45] These findings imply the functions of DDX5 in transcription (both transcription initiation and termination), DNA repair, and genome maintenance via R-loops regulation.

On the other hand, the present work suggests the dual functions of DDX5 in transcription and DNA damage response that can be achieved through DDX5 interaction with the multifunctional transcription initiation (TFIIH) complex and the Ku DNA end-binding proteins. There are many lines of scientific evidence supporting a cross-talk between transcription and DNA repair via a set of common molecular utilized networks such as the TFIIH core subunit XPB[46,47] and the Ku70/80 complex that has been recently reported to bind to the promoter DNA region and interact with transcription factors for transcriptional modulation.[48,49]

Emma L. Clark et al. pointed out that DDX5 functions as a "coupling" factor, coordinating both transcription and RNA processing of AR-regulated genes in PC.[15] In consistency with this finding, our DDX5 PPI revealed the tight connection between DDX5 and the core proteins of the basal initiation transcription factor complex TFIIH playing a role in transcription of protein-coding genes mediated by RNA Pol II.[47] Several protein subunits of the transcription factor IIIC complex and the RNAP (RNA polymerase) were obtained in the DDX5 interactome of CR cells. Noticeably, our data also showed a group of transcription factors that appeared as DDX5 interacting proteins (data not shown). In the absence of AR-negative CR cells, cellular survival and growth are driven by bypass pathways, including increased activity of MAPK, PI3K, and PCK cascade and aberrant expression and activity of oncogenes (such as BCL2). DDX5 could participate in expression regulation of these oncogenes by coordination with other transcription factors, transcriptional machinery, and RNA-processing proteins, thereby contributing to CRPC development.

Collectively, the oncogenic functions of DDX5 in PC that are described in the present work and previous reports allow us to paint a hypothesis

Figure 4. Functional bioinformatics analyzing DDX5 interaction proteins identified in the study

(A) The pie chart shows the proportion of the novel DDX5-interacting proteins (87.9%) and the identified interactions characterized as known DDX5-interacting proteins in the string database (12.1%). (B) Gene ontology biological process (GO-BP) enrichment analyses of the DDX5 interactome were performed using BiNGO (hypergeometric test, Benjamini and Hochberg false discovery rate [FDR] correction, p = 0.005, biological process). The bar chart shows the top functions ranked by the fold enrichment score. (C) CORUM enrichment analysis allows identifying experimentally proven human protein complexes associated with DDX5. (D) Network modeling of the top enriched protein complexes and DDX5. Green nodes represent proteins found in the DDX5 interactome obtained in the study, while gray nodes mean proteins were not identified. Bordered edges represent interactions with DDX5 annotated in published PPI databases. All of the protein members of the IGF2BP1 complex were found in the DDX5 interactions. A solid connection between DDX5 and the toposome was observed since most of the protein components of the toposome associate with DDX5 in the study (SSRP1 did not appear in the DDX5 interactions, but it was annotated to interact with DDX5 in string db). We showed the rigid association of DDX5 with the general transcription factor complex GTFIIH (or TFIIH), which is composed of the core complex (GTF2H1, GTF2H2, GTF2H3, GTF2H4, ERCC2, ERCC3) and the CAK (CDK7, CCNH, MNAT1). DDX5 could modulate transcription through the 7SK RPN complex because all of its constructive proteins (CDK9, HEXIM1, CCNT1, and LARP7) interact with DDX5.

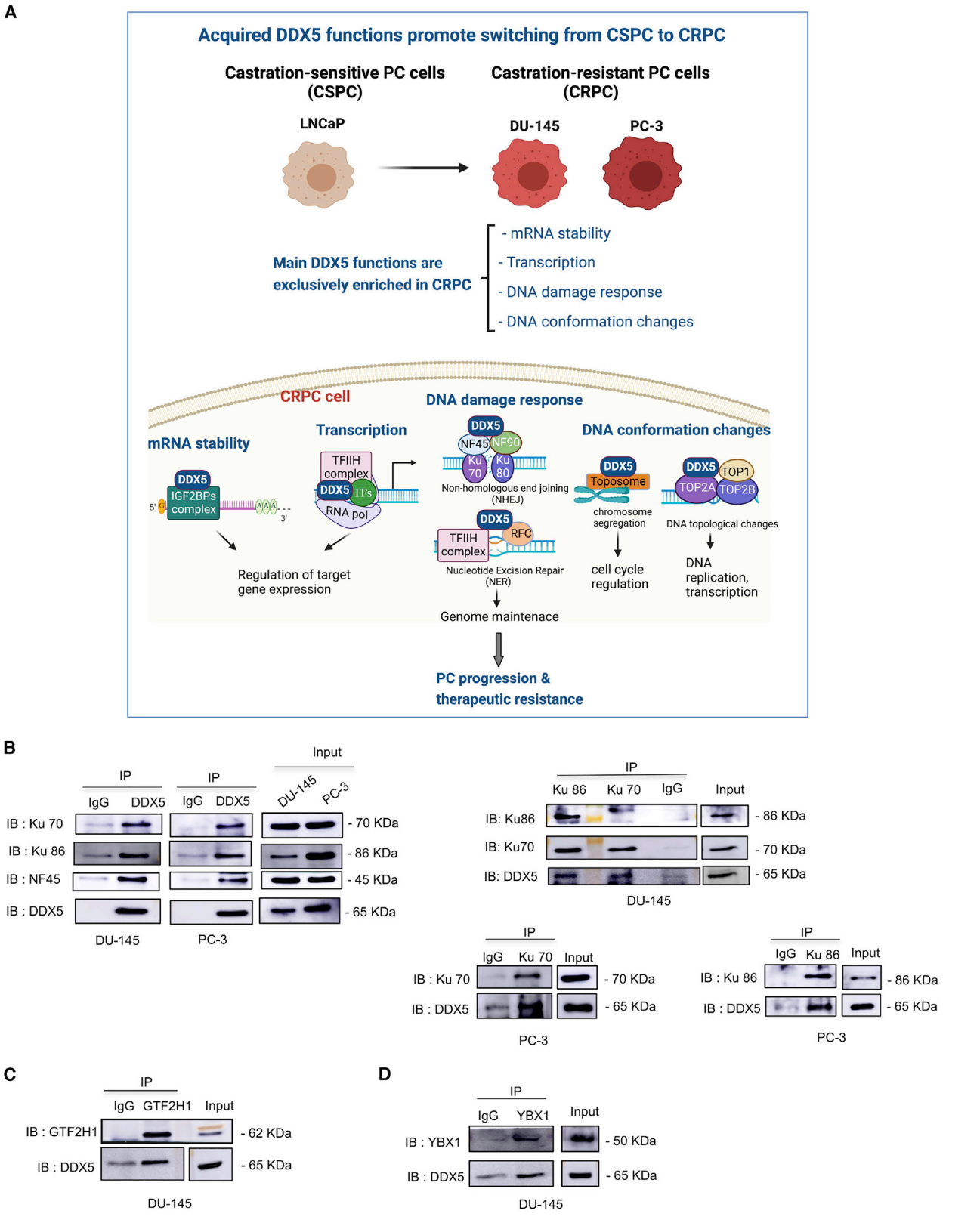

(legend on next page)

Table 1. List of DDX5 interacting proteins implicated in the DNA damage response identified in four PC cell lines

Proteins	PNT1A	LNCaP	DU-145	PC-3	DDR-related pathways
XRCC6			x	x	NHEJ
XRCC5			x	x	NHEJ
GTF2H4			x	x	NER
GTF2H1			x	x	NER
ERCC3			x	x	NER
GTF2H2			x	x	NER
GTF2H3			x	x	NER
RFC5		x	x	x	NER
UPF1			x	x	Unclear
PRPF19			x	x	NER, NHEJ
IGHMBP2			x	x	Unclear
MSH6		x	x		MR
TP53			x		BER, NER, DSBR, mitochondrial DNA repair
LIG3			x		BER, NER, alNHEJ, HR, mitochondrial DNA repair
RFC3			x		NER
ERCC2			x		NER
ERCC6				x	NER
RFC1				x	NER
TOP2A				x	DDR
RECQL4				x	HR
MRPS26				x	Mitochondrial DNA repair
MRPS35				x	Mitochondrial DNA repair
DTX3L				x	NHEJ

DDR, DNA damage response; DSBR, double-strand break repair; NHEJ, non-homologous end joining; HR, homologous recombination; MR, mismatch repair; BER, base excision repair; NER, nucleotide excision repair.

picture of how DDX5 can promote CRPC by playing as a cross-talk among different signaling pathways such as transcription, RNA processing, and DNA repair. Without any therapeutics, DDX5 regulates R-loop structure, recruits and/or associates with RNAPII, TFIIH, and other transcription factors, and participates in coupling transcription-RNA process, thereby facilitating transcription process, avoiding DNA damages, and maintaining genome integrity. On the other hand, upon DNA lesion-inducing-treatments, DDX5 can immediately facilitate DNA repair at the active transcription sites either via clearing of RNA transcripts of R-loop or enhancing the recruitment and/or activity of the DNA repair machinery (Ku complex, TFIIH complex), ensuring proper and prompt DNA repair, thereby maintaining genomic stability and enhancing tolerance of cancer cells to therapies (Figure 7).

In summary, treatment options of CRPC that progress after chemotherapy remain challenging. Here, we show the translational significance of DDX5 silencing using ASO technology that could be represented as a new therapeutic strategy in CRPC. DDX5 overexpression is linked to CRPC progression, and DDX5 can promote disease evolution through participating in various critical cellular processes, notably in the DNA damage response. Our worldwide-patented ASO targeting DDX5 could have potential to be highly impactful in combating CRPC, particularly in the setting of CRPC progressing after docetaxel treatment, as a monotherapy or more probably in combination with other approaches including other chemotherapies or therapeutic radiation (e.g., PSMA-directed radionuclide therapy). Additionally, this ASO-directed DDX5 mRNA silencing could be operative in other cancer types in which DDX5 acts as a major oncogenic player. Further works will focus on evaluating toxicologic and pharmacologic properties of the DDX5 ASO.

MATERIALS AND METHODS

Cell lines and cell culture conditions

Four different human prostate cell lines were used as a way to study PC pathogenesis: normal phenotype cell PNT1A (NM, ECACC, European Collection of Cell Cultures, England), CS LNCaP (ATCC, American Type Culture Collection, Rockville, MD, USA), and CR DU-145 and PC-3 cell lines (ATCC). Additionally, two LNCaP-derived cell lines were used, LNCaP overexpressing Hsp27 (LNCaP-Hsp27) and LNCaP-mock (empty vector), which were established as previously described.[7] The cells were maintained with either the RPMI-1640 medium (Roswell Park Memorial Institute) (for PNT1A, LNCaP, LNCaP-mock, and LNCaP-Hsp27) or DMEM medium (Dulbecco's Modified Eagle's Medium) (for PC-3 and DU-145), supplemented with 10% fetal bovine serum at 37°C in 5% CO_2.

Figure 5. Acquired DDX5 functions lead to switching from castration sensitivity to castration resistance of PC

(A) The scheme describes the hypothesis about how DDX5 can promote PC progression and therapeutic resistance based on functional analyses of DDX5 interaction network. DDX5 could drive PC progression and therapeutic resistance through playing roles in DNA damage response, mRNA stabilization, transcription, and DNA conformation changes since these cellular processes are exclusively enriched in the DDX5 PPI obtained in CRCP. In particular, DDX5 regulates mRNA stability via interacting with IGF2BP complex, thereby modulating expression of target genes. DDX5 also regulates gene expression by monitoring transcription initiation via associating with the basal transcription complex TFIIH and transcription factors (TFs). DDX5 functions in non-homologous end joining (NHEJ) via interacting with the Ku70/Ku80 and NF45/NF90 complexes. DDX5 also interacts with the TFIIH complex and RFC proteins (RFC1, RFC3, RFC5) to participate in nucleotide excision repair (NER). DDX5 may regulate the cell cycle through its interaction with the toposome complex acting in chromosome segregation. Through binding to different topoisomerase enzymes such as TOP2A, TOP2B, and TOP1, DDX5 can modulate the DNA topological changes, thereby monitoring DNA replication and transcription. (B) IP using anti-DDX5 Ab followed by WB with anti-Ku70 Ab, anti-Ku80 Ab, and anti-NF45 Ab shows the presence of Ku70, Ku80, and NF45 in the DDX5 complexes in both CR DU-145 and PC-3 cells (left above panel). The reverse IP using anti-Ku70 Ab and anti- Ku80 Ab followed by WB using anti-DDX5 Ab confirmed the interaction of DDX5 with the Ku70/Ku80 heterodimer (right above and below panel). (C and D) Similarly, the IP using anti-GTF2H1 Ab and anti-YBX1 Ab combined with WB using anti-DDX5 Ab confirmed the association of DDX5 with GTF2H1 (C) and YBX1 (D).

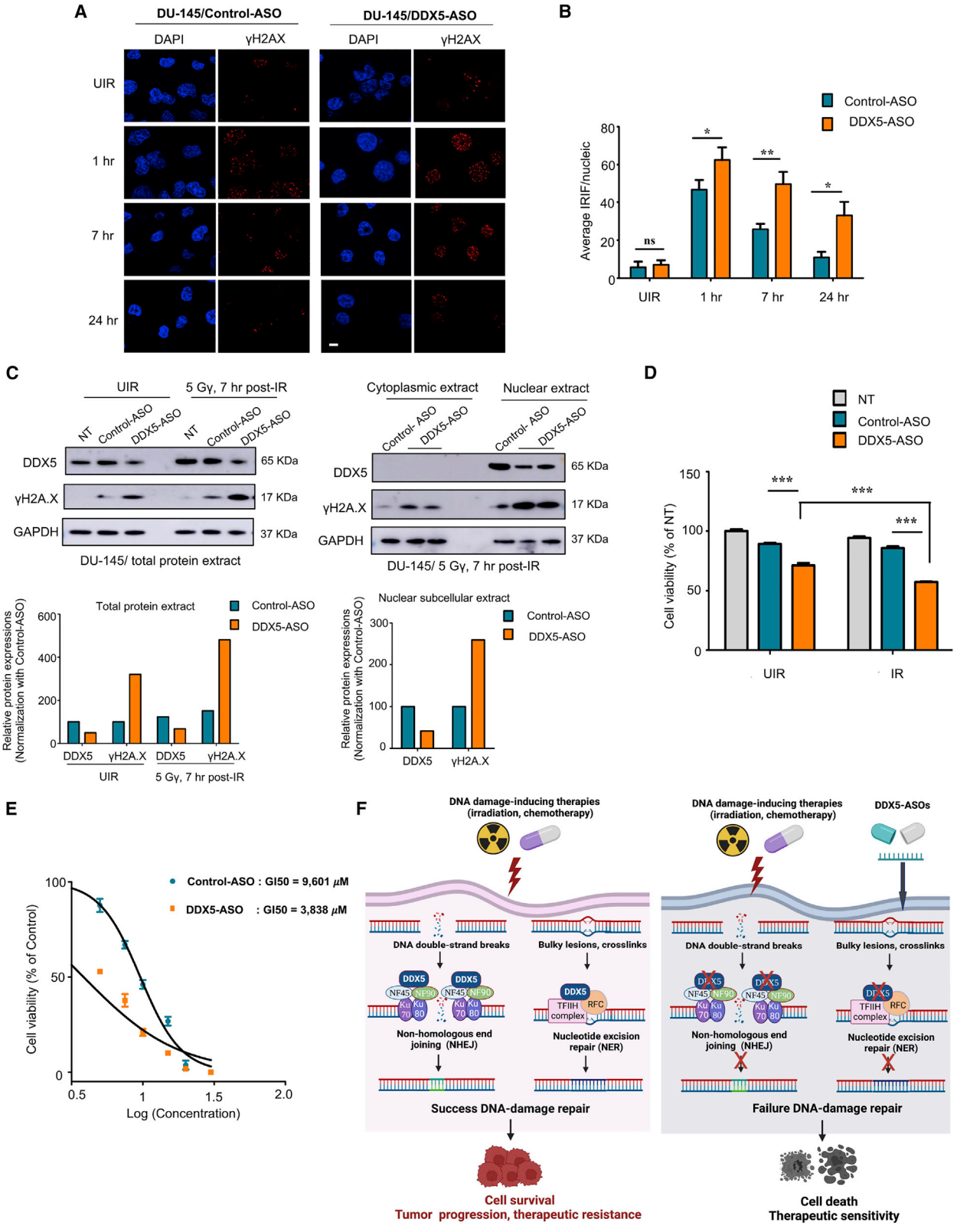

(legend on next page)

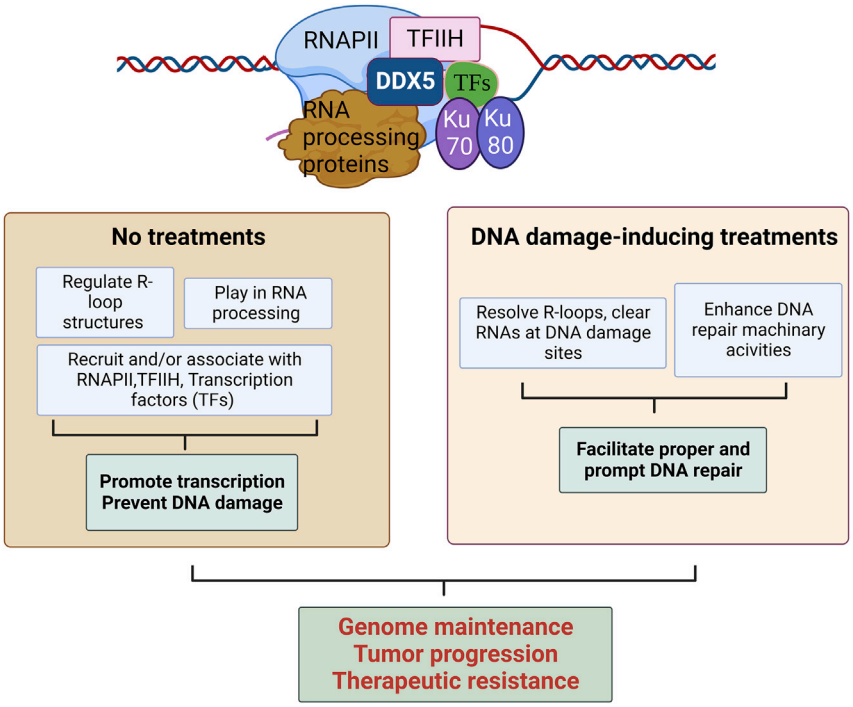

Figure 7. The scheme illustrates a hypothesis picture of how DDX5 can promote tumor progression and therapeutic resistance via playing as a cross-talk among different signaling pathways such as transcription, RNA processing, and DNA repair in CRPC

The increased R-loop formation frequently occurs in accessible chromatin regions of highly transcribed genes located in gene-rich areas that are more sensitive to DNA damage-inducing therapies than the other parts of the genome. Without any treatments, DDX5 mediates R-loops structure, recruits and/or binds with RNAPII, transcription initiation complex (TFIIH), and other transcription factors (TFs), and participates in coupling transcription-RNA process, thereby facilitating transcription process, preventing DNA damages, and promoting tumor development. On the other hand, upon DNA damage-inducing therapies, DDX5 can immediately facilitate DNA repair at the active transcription sites either via clearance of RNA transcripts of R-loop or enhancing the recruitment and/or activity of the DNA repair machinery (Ku complex, TFIIH complex), ensuring proper and rapid DNA repair, resulting in genomic maintenance and tolerance enhancement of cancer cells to therapies.

Human prostate cancer TMA construction and immunohistochemistry

A TMA containing 515 specimens (79 benign prostate hyperplasia, 266 untreated primary [hormone naive] tumors, 113 NHT tumors, 57 CRPCs) was obtained from the Vancouver Prostate Center Tissue Bank. Except CRPC samples that were obtained via transurethral resection of the prostate, all specimens were collected through radical prostatectomy. IHC staining was performed by Dr. Ladan Fazli with mouse anti-DDX5 monoclonal antibody (sc-365164, Santa Cruz Biotechnology, CA, USA) using the Ventana autostainer (model Discover XT; Ventana Medical System, Tucson, AZ) with an enzyme-labeled biotin-streptavidin system and a solvent-resistant DAB Map kit (Ventana). DDX5 staining intensity was scored using Aperio/Leica software called ImageScope. The image analyzing process was done by applying IHC (intensity and pixel count) scoring algorithms directly to the annotated area in the scanned image.

ASO design, selection, and transfection in PC cells

Synthesis of DDX5-targeting ASOs was performed in Optoligo, a French Inserm Transfert-sponsored platform. ASOs were designed using a computational algorithm developed in our laboratory by P.F. First, the coding part of the DDX5 mRNA sequence (NM_001320595.2) was selected and divided into a set of consecutive sequences that contained 20 base pairs. The resulting sequences were converted into their complementary acid nucleotide sequences, which were subsequently inverted to obtain the potential ASO sequences. The ASO sequences were individually evaluated regarding their GC content and their specificity using NCBI's Basic Local Alignment Search Tool (BLAST), with the use of the "blastn" algorithm and the NCBI reference transcript database "refseq_rna" as parameters. The ultimate selection was done manually by excluding all ASOs showing sequence similarities with other genes. The lead ASOs were synthesized in our laboratory by C.P. following a previously described procedure.[50] These ASOs had been modified with a phosphorothioate backbone that protected

Figure 6. DDX5 promotes therapeutic resistance of CRPC through activation of DNA repair

(A and B) DDX5 downregulation reduces DNA damage repair efficiency by immunofluorescent (IF) and irradiation induced foci (IRIF) counting. The DU-145 cells were transfected with 150 nM DDX5-ASO (hmASO3) or control-ASO, and 3 days later, the cells were exposed to 5 Gy IR and further cultured for various time periods (UIR = unirradiated, 1, 7, and 24 h). IF staining using anti-γH2AX antibody was carried out (A). The graph shows a higher number of the IRIF in DDX5-ASO-treated cells compared with the control-ASO-transfected cells (B). (C) WB analysis shows that DDX5 depletion defects the DNA repair process. DU-145 cells transfected with the DDX5-ASO (hmASO3) or control-ASO (150 nM) were exposed to 5 Gy IR and further cultured for 7 h. The total protein extract or compartment extracts including cytoplasmic and nuclear extracts were subjected to WB analysis using anti-DDX5 Ab, anti-γH2AX Ab, and GAPDH used as a loading control. (D and E) DDX5 knockdown enhances cell sensitivity to DNA damage stress stimuli such as irradiation (D) and cisplatin (E). The DU-145 cells were transfected with DDX5-ASO for 2 days, treated with either irradiation or cisplatin, and subjected to cell proliferation evaluation using MTT assay after 2 days. The MTT tests were performed with triplication. DDX5-ASO can lower GI_{50} of cisplatin up to nearly three times. (F) In DDX5-overexpressed PC cells, DDX5 facilitates two main DNA repair pathways (NHEJ, NER), ensuring the proper DNA repair upon DNA damage-inducing therapies such as irradiation and chemotherapy, thereby promoting cell survival, PC development, and therapeutic resistance (left panel). Conversely, DDX5-downregulated PC cells failed to repair DNA lesions; therefore, they are sensitive to treatments (right panel). *$p < 0.05$; **$p < 0.01$; ***$p < 0.001$; ns, non-significant.

them against degradation by nucleases. The ASOs alter targeted mRNA through RNase H1-mediated RNA cleavage.

Cells (at ~50% density) were transfected with ASOs two times as previously described.[50] ASOs were pre-incubated with 1 mL Gibco Opti-MEM (Life Technologies, Courtaboeuf, France) containing 4 uL Oligofectamine (Life Technologies, Courtaboeuf, France) for 20–30 min before adding to the cells. After 4 h, the mixture of ASOs and Oligofectamine was removed, and the fresh completed medium was supplied. The ASO treatment was repeated exactly the same on the following day. After 3 days, the transfected cells were harvested for protein extraction and western blot analysis. The protein expression was evaluated quantitatively using ImageJ (NIH) software.

The hmASO3 was patented worldwide by Inserm Transfer with the PATENT N.REF as PCT/EP2020/082548 (WO2021099394A1, 2021).

Preclinical evaluation of ASO treatment in PC-3 xenografts

PC-3 cells (10×10^6) in 100 μL DBPS 1X were inoculated subcutaneously in the right flank of 5-week-old male BALB/c nude mice (Charles River Laboratories, France). After 12 days, the tumors reached from 50 to 100 mm^3, and the treatment started on the next day. Mice (n = 14) were randomly selected for treatment with DDX5- or control-ASO. Each group received daily intraperitoneal injection of 12.5 mg/kg DDX5- or control-ASO for 5 weeks. Tumor volume (mm^3) was measured weekly using a caliper in three perpendicular dimensions (X = width, Y= length, Z = depth), and calculated following the formula $X \times Y \times Z \times 0.5236$. During the period of treatment, the mice were observed for signs of systemic toxicity, and their body weights were recorded daily too. The mice were maintained in an animal facility (agreement #13.2700). P.R. owns a personal agreement (#A13-477) for the animal handling and experimentation for this study. Animal experimentation was performed following ethics laws recommendations.

Western blot analysis

WB experiments were carried our following the described procedure.[50] The membranes were incubated with the primary antibodies including vinculin and GAPDH as loading controls (supplemental information, Table S6). The primary Abs were probed with the corresponding HRP-conjugated secondary Abs (DAKO, Agilent, United States) and detected using ECL Prime Western Blotting detection reagent (RPN2236, GE Healthcare, Vélizy-Villacoublay, France). The images were captured using the Amersham Imager 680 blot and gel imager (GE Healthcare, Vélizy-Villacoublay, France).

Immunofluorescence for DNA damage foci formation

The DU-145 cells were cultured on coverslips. After 3 days of transfection with the DDX5 ASO as described above, the cells were irradiated using RS-2000X-RayIrradiator (Rab Source Technology, USA). Subsequently, the cells were fixed in 4% (wt/vol) paraformaldehyde for 15 min, permeabilized with 0.1% Triton X-100 in 1X PBS for 15 min, and blocked with 5% (wt/vol) BSA for 30 min, at room temperature (RT). The samples were then incubated overnight at 4°C with primary antibody against p-γH2AX, followed by 1-h incubation at RT with a secondary fluorescein isothiocyanate anti-rabbit antibody (Alexa Fluor 488, Thermo Fisher Scientific, Life Technologies, Villebon-sur-Yvette, France). Nuclei were stained with DAPI (4′, 6-diamidino-2-phenylindole) and coverslips were mounted with ProLong Gold Antifade Mountant (Thermo Fisher Scientific, Life Technologies, Villebon-sur-Yvette, France). Images were captured using Apotome (Zeiss, Le Pecq, France).

Bioinformatics analyses

The DDX5-interacting proteins found in four cell lines were functionally classified using PANTHER 14.1.[51] Analysis of GO enrichment used BiNGO tool run by Cytoscape[52] with the statistical test "Hypergeometric test," and Benjamini and Hochberg FDR correction, two significant levels p = 0.05 and p = 0.005, and the whole annotation as a reference set. Analysis of protein complexes enrichment was performed using Gprofiler[53] for CRORUM 3.0 database (https://mips.helmholtz-muenchen.de/corum/), which collects annotation of mammalian protein complexes obtained from manual experiments[54] with threshold p = 0.05. To compare the GO enrichment analysis results among four DDX5 interactomes from four cell lines, the ClusterProfiler R packages[55] were used. *DDX5* mRNA expression was extracted form TCGA PRAD RNAseq public data (https://portal.gdc.cancer.gov/projects/TCGA-PRAD). *DDX5* in 498 tumor samples (T) was measured as discrete values after comparison with median expression in 52 normal prostate samples (N): upregulation, thereafter designated "*DDX5* high," was defined by a T/N ratio ≥ 1 and no upregulation ("*DDX5* low") by a T/N ratio <1.

Statistical analysis

All pooled results are represented as mean ± SEM. Statistical analyses were carried out using GraphPad Prism 6 software (GraphPad Software). The independent sample t test was performed to compare means between two groups. RFS from TCGA PRAD samples was calculated from the date of diagnosis until the date of relapse. Follow-up was measured from the date of diagnosis to the date of last news for event-free patients. Results with $p < 0.05$ were considered statistically significant and are indicated by *$p < 0.05$; **$p < 0.01$; ***$p < 0.001$, and ****$p < 0.0001$.

DATA AVAILABILITY

Protein interaction AP-MS data: PRIDE PXD023252 (http://www.ebi.ac.uk/pride/archive/projects/PXD023252).

SUPPLEMENTAL INFORMATION

Supplemental information can be found online at https://doi.org/10.1016/j.ymthe.2022.08.005.

ACKNOWLEDGMENTS

We give special thanks to the Experimental Histo-Pathology platform (IPC/CRCM Experimental Pathology or ICEP) for the help with Ki67 immunohistological staining, to Dr. Pauline BRIGE (European

Center for Research in Medical Imaging, Aix-Marseille University) for her help with the Ki67 staining analysis, and to Mr. DUONG Quang Hieu (M2 student, Inserm UMR 1068, CNRS UMR 7258, Institut Paoli-Calmettes, Aix-Marseille University) for his support with western blot analysis during the revision.

This work was supported by Inserm and grants from ITMO Cancer (BioSys call, #A12171AS) and the Amidex Fondation "Emergence & Innovation" project (NucleoTHER). T.K.L.'s fellowship was funded by the 911 project-Vietnam International Education Department (VIED). Proteomic analyses were done using the mass spectrometry facility of Marseille Proteomics (marseille-proteomique.univ-amu.fr) supported by IBiSA (Infrastructures Biologie Santé et Agronomie).

AUTHOR CONTRIBUTIONS

T.K.L., D.T., and P.R. conceived this project; T.K.L., C.C., K.O., C.P., F.R., S.A., E.B., and L.F. performed and analyzed the experiments; T.K.L., M.H., D.B., P.F., and C.B. performed bioinformatics analyses; D.T., P.R., M.G., and F.B. gave critical comments; T.K.L. wrote the manuscript with the approval of all other authors.

DECLARATION OF INTERESTS

The authors declare to have no financial, personal, or professional competing interest and no conflict of interest.

REFERENCES

1. Bray, F., Ferlay, J., Soerjomataram, I., Siegel, R.L., Torre, L.A., and Jemal, A. (2018). Global cancer statistics 2018: GLOBOCAN estimates of incidence and mortality worldwide for 36 cancers in 185 countries. CA. Cancer J. Clin. *68*, 394–424.

2. Katsogiannou, M., Ziouziou, H., Karaki, S., Andrieu, C., Henry de Villeneuve, M., and Rocchi, P. (2015). The hallmarks of castration-resistant prostate cancers. Cancer Treat. Rev. *41*, 588–597.

3. Rocchi, P., Jugpal, P., So, A., Sinneman, S., Ettinger, S., Fazli, L., Nelson, C., and Gleave, M. (2006). Small interference RNA targeting heat-shock protein 27 inhibits the growth of prostatic cell lines and induces apoptosis via caspase-3 activation in vitro. BJU Int. *98*, 1082–1089.

4. Rocchi, P., Beraldi, E., Ettinger, S., Fazli, L., Vessella, R.L., Nelson, C., and Gleave, M. (2005). Increased Hsp27 after androgen ablation facilitates androgen-independent progression in prostate cancer via signal transducers and activators of transcription 3-mediated suppression of apoptosis. Cancer Res. *65*, 11083–11093.

5. Rocchi, P., So, A., Kojima, S., Signaevsky, M., Beraldi, E., Fazli, L., Hurtado-Coll, A., Yamanaka, K., and Gleave, M. (2004). Heat shock protein 27 increases after androgen ablation and plays a cytoprotective role in hormone-refractory prostate cancer. Cancer Res. *64*, 6595–6602.

6. Andrieu, C., Taieb, D., Baylot, V., Ettinger, S., Soubeyran, P., De-Thonel, A., Nelson, C., Garrido, C., So, A., Fazli, L., et al. (2010). Heat shock protein 27 confers resistance to androgen ablation and chemotherapy in prostate cancer cells through eIF4E. Oncogene *29*, 1883–1896.

7. Baylot, V., Katsogiannou, M., Andrieu, C., Taieb, D., Acunzo, J., Giusiano, S., Fazli, L., Gleave, M., Garrido, C., and Rocchi, P. (2012). Targeting TCTP as a new therapeutic strategy in castration-resistant prostate cancer. Mol. Ther. *20*, 2244–2256.

8. Cherif, C., Nguyen, D.T., Paris, C., Le, T.K., Sefiane, T., Carbuccia, N., Finetti, P., Chaffanet, M., Kaoutari, A.E., Vernerey, J., et al. (2022). Menin inhibition suppresses castration-resistant prostate cancer and enhances chemosensitivity. Oncogene *41*, 125–137.

9. Cohen, A.A., Geva-Zatorsky, N., Eden, E., Frenkel-Morgenstern, M., Issaeva, I., Sigal, A., Milo, R., Cohen-Saidon, C., Liron, Y., Kam, Z., et al. (2008). Dynamic proteomics of individual cancer cells in response to a drug. Science *322*, 1511–1516.

10. Nyamao, R.M., Wu, J., Yu, L., Xiao, X., and Zhang, F.-M. (2019). Roles of DDX5 in the tumorigenesis, proliferation, differentiation, metastasis and pathway regulation of human malignancies. Biochim. Biophys. Acta Rev. Cancer *1871*, 85–98.

11. Fuller-Pace, F.V. (2006). DExD/H box RNA helicases: multifunctional proteins with important roles in transcriptional regulation. Nucleic Acids Res. *34*, 4206–4215.

12. Bond, A.T., Mangus, D.A., He, F., and Jacobson, A. (2001). Absence of Dbp2p alters both nonsense-mediated mRNA decay and rRNA processing. Mol. Cel. Biol. *21*, 7366–7379.

13. Wagner, M., Rid, R., Maier, C.J., Maier, R.H., Laimer, M., Hintner, H., Bauer, J.W., and Onder, K. (2012). DDX5 is a multifunctional co-activator of steroid hormone receptors. Mol. Cel. Endocrinol. *361*, 80–91.

14. Wang, Z., Luo, Z., Zhou, L., Li, X., Jiang, T., and Fu, E. (2015). DDX5 promotes proliferation and tumorigenesis of non-small-cell lung cancer cells by activating β-catenin signaling pathway. Cancer Sci. *106*, 1303–1312.

15. Clark, E.L., Hadjimichael, C., Temperley, R., Barnard, A., Fuller-Pace, F.V., and Robson, C.N. (2013). p68/DdX5 supports β-catenin & RNAP II during androgen receptor mediated transcription in prostate cancer. PLOS ONE *8*, e54150.

16. Nicol, S.M., Bray, S.E., Black, H.D., Lorimore, S.A., Wright, E.G., Lane, D.P., Meek, D.W., Coates, P.J., and Fuller-Pace, F.V. (2013). The RNA helicase p68 (DDX5) is selectively required for the induction of p53-dependent p21 expression and cell cycle arrest after DNA damage. Oncogene *32*, 3461–3469.

17. Guturi, K.K.N., Sarkar, M., Bhowmik, A., Das, N., and Ghosh, M.K. (2014). DEAD-box protein p68 is regulated by β-catenin/transcription factor 4 to maintain a positive feedback loop in control of breast cancer progression. Breast Cancer Res. *16*, 496.

18. Clark, E.L., Coulson, A., Dalgliesh, C., Rajan, P., Nicol, S.M., Fleming, S., Heer, R., Gaughan, L., Leung, H.Y., Elliott, D.J., et al. (2008). The RNA helicase p68 is a novel androgen receptor coactivator involved in splicing and is overexpressed in prostate cancer. Cancer Res. *68*, 7938–7946.

19. Taniguchi, T., Iizumi, Y., Watanabe, M., Masuda, M., Morita, M., Aono, Y., Toriyama, S., Oishi, M., Goi, W., and Sakai, T. (2016). Resveratrol directly targets DDX5 resulting in suppression of the mTORC1 pathway in prostate cancer. Cell Death Dis. *7*, e2211.

20. You, Z., Liu, C., Wang, C., Ling, Z., Wang, Y., Wang, Y., Zhang, M., Chen, S., Xu, B., Guan, H., and Chen, M. (2019). LncRNA CCAT1 promotes prostate cancer cell proliferation by interacting with DDX5 and MIR-28-5P. Mol. Cancer Ther. *18*, 2469–2479.

21. Causevic, M., Hislop, R.G., Kernohan, N.M., Carey, F.A., Kay, R.A., Steele, R.J., and Fuller-Pace, F.V. (2001). Overexpression and poly-ubiquitylation of the DEAD-box RNA helicase p68 in colorectal tumours. Oncogene *20*, 7734–7743.

22. Mooney, S.M., Grande, J.P., Salisbury, J.L., and Janknecht, R. (2010). Sumoylation of p68 and p72 RNA helicases affects protein stability and transactivation potential. Biochemistry *49*, 1–10.

23. Bernard, A., Kimko, H., Mital, D., and Poggesi, I. (2012). Mathematical modeling of tumor growth and tumor growth inhibition in oncology drug development. Expert Opin. Drug Metab. Toxicol. *8*, 1057–1069.

24. Wilson, B.J., and Giguère, V. (2007). Identification of novel pathway partners of p68 and p72 RNA helicases through Oncomine meta-analysis. BMC Genomics *8*, 419.

25. Yang, J., Zhao, Y., Kalita, M., Li, X., Jamaluddin, M., Tian, B., Edeh, C.B., Wiktorowicz, J.E., Kudlicki, A., and Brasier, A.R. (2015). Systematic determination of human cyclin dependent kinase (CDK)-9 interactome identifies novel functions in RNA splicing mediated by the DEAD box (DDX)-5/17 RNA helicases. Mol. Cel. Proteomics *14*, 2701–2721.

26. Roberts, T.C., Langer, R., and Wood, M.J.A. (2020). Advances in oligonucleotide drug delivery. Nat. Rev. Drug Discov. *19*, 673–694.

27. Kulkarni, J.A., Witzigmann, D., Thomson, S.B., Chen, S., Leavitt, B.R., Cullis, P.R., and van der Meel, R. (2021). The current landscape of nucleic acid therapeutics. Nat. Nanotechnol. *16*, 630–643.

28. Le, T.K., Paris, C., Khan, K.S., Robson, F., Ng, W.-L., and Rocchi, P. (2021). Nucleic acid-based technologies targeting coronaviruses. Trends Biochem. Sci. *46*, 351–365.

29. Capasso, A., Bagby, S.M., Dailey, K.L., Currimjee, N., Yacob, B.W., Ionkina, A., Frank, J.G., Kim, D.J., George, C., Lee, Y.B., et al. (2019). First-in-Class phosphorylated-p68

inhibitor RX-5902 inhibits β-catenin signaling and demonstrates antitumor activity in triple-negative breast cancer. Mol. Cancer Ther. *18*, 1916–1925.

30. Berman, A.Y., Motechin, R.A., Wiesenfeld, M.Y., and Holz, M.K. (2017). The therapeutic potential of resveratrol: a review of clinical trials. NPJ Precis. Oncol. *1*, 35.
31. Mancarella, C., and Scotlandi, K. (2019). IGF2BP3 from physiology to cancer: novel discoveries, unsolved issues, and future perspectives. Front. Cel Dev. Biol. *7*, 363.
32. Bates, M., Boland, A., McDermott, N., and Marignol, L. (2020). YB-1: the key to personalised prostate cancer management? Cancer Lett. *490*, 66–75.
33. Shiota, M., Fujimoto, N., Imada, K., Yokomizo, A., Itsumi, M., Takeuchi, A., Kuruma, H., Inokuchi, J., Tatsugami, K., Uchiumi, T., et al. (2016). Potential role for YB-1 in castration-resistant prostate cancer and resistance to enzalutamide through the androgen receptor V7. J. Natl. Cancer Inst. *108*, djw005.
34. Gordon, S., Akopyan, G., Garban, H., and Bonavida, B. (2006). Transcription factor YY1: structure, function, and therapeutic implications in cancer biology. Oncogene *25*, 1125–1142.
35. Stovall, D.B., and Sui, G. (2013). The Function of YY1 and its Oncogenic Role in Prostate Cancer (IntechOpen).
36. Oh, S., Oh, C., and Yoo, K.H. (2017). Functional roles of CTCF in breast cancer. BMB Rep. *50*, 445–453.
37. Chappell, W.H., Lehmann, B.D., Terrian, D.M., Abrams, S.L., Steelman, L.S., and McCubrey, J.A. (2012). p53 expression controls prostate cancer sensitivity to chemotherapy and the MDM2 inhibitor Nutlin-3. Cell Cycle *11*, 4579–4588.
38. Bader, A.S., Hawley, B.R., Wilczynska, A., and Bushell, M. (2020). The roles of RNA in DNA double-strand break repair. Br. J. Cancer *122*, 613–623.
39. Cargill, M., Venkataraman, R., and Lee, S. (2021). DEAD-box RNA helicases and genome stability. Genes *12*, 1471.
40. Lu, W.-T., Hawley, B.R., Skalka, G.L., Baldock, R.A., Smith, E.M., Bader, A.S., Malewicz, M., Watts, F.Z., Wilczynska, A., and Bushell, M. (2018). Drosha drives the formation of DNA:RNA hybrids around DNA break sites to facilitate DNA repair. Nat. Commun. *9*, 532–613.
41. Yu, Z., Mersaoui, S.Y., Guitton-Sert, L., Coulombe, Y., Song, J., Masson, J.-Y., and Richard, S. (2020). DDX5 resolves R-loops at DNA double-strand breaks to promote DNA repair and avoid chromosomal deletions. NAR Cancer *2*, zcaa028.
42. Mersaoui, S.Y., Yu, Z., Coulombe, Y., Karam, M., Busatto, F.F., Masson, J.-Y., and Richard, S. (2019). Arginine methylation of the DDX5 helicase RGG/RG motif by PRMT5 regulates resolution of RNA:DNA hybrids. EMBO J. *38*, e100986.
43. Cristini, A., Groh, M., Kristiansen, M.S., and Gromak, N. (2018). RNA/DNA hybrid interactome identifies DXH9 as a molecular player in transcriptional termination and R-loop-associated DNA damage. Cell Rep. *23*, 1891–1905.
44. Villarreal, O.D., Mersaoui, S.Y., Yu, Z., Masson, J.-Y., and Richard, S. (2020). Genome-wide R-loop analysis defines unique roles for DDX5, XRN2, and PRMT5 in DNA/RNA hybrid resolution. Life Sci. Alliance *3*, e202000762.
45. Sessa, G., Gómez-González, B., Silva, S., Pérez-Calero, C., Beaurepere, R., Barroso, S., Martineau, S., Martin, C., Ehlén, Å., and Martínez, J.S. (2021). BRCA2 promotes DNA-RNA hybrid resolution by DDX5 helicase at DNA breaks to facilitate their repair‡. EMBO J. *40*, e106018.
46. Compe, E., and Egly, J.-M. (2012). TFIIH: when transcription met DNA repair. Nat. Rev. Mol. Cel Biol. *13*, 343–354.
47. Rimel, J.K., and Taatjes, D.J. (2018). The essential and multifunctional TFIIH complex. Protein Sci. *27*, 1018–1037.
48. Shi, L., Qiu, D., Zhao, G., Corthesy, B., Lees-Miller, S., Reeves, W.H., and Kao, P.N. (2007). Dynamic binding of Ku80, Ku70 and NF90 to the IL-2 promoter in vivo in activated T-cells. Nucleic Acids Res. *35*, 2302–2310.
49. Sucharov, C.C., Helmke, S.M., Langer, S.J., Perryman, M.B., Bristow, M., and Leinwand, L. (2004). The Ku protein complex interacts with YY1, is up-regulated in human heart failure, and Represses α myosin heavy-chain gene expression. Mol. Cel. Biol. *24*, 8705–8715.
50. Nguyen, D.T., Le, T.K., Paris, C., Cherif, C., Audebert, S., Udu-Ituma, S.O., Benizri, S., Barthélémy, P., Bertucci, F., Taïeb, D., and Rocchi, P. (2021). Antisense oligonucleotide-based therapeutic against menin for triple-negative breast cancer treatment. Biomedicines *9*, 795.
51. Mi, H., Muruganujan, A., Casagrande, J.T., and Thomas, P.D. (2013). Large-scale gene function analysis with the PANTHER classification system. Nat. Protoc. *8*, 1551–1566.
52. Maere, S., Heymans, K., and Kuiper, M. (2005). BiNGO: a Cytoscape plugin to assess overrepresentation of gene ontology categories in biological networks. Bioinformatics *21*, 3448–3449.
53. Raudvere, U., Kolberg, L., Kuzmin, I., Arak, T., Adler, P., Peterson, H., and Vilo, J. (2019). g:Profiler: a web server for functional enrichment analysis and conversions of gene lists (2019 update). Nucleic Acids Res. *47*, W191–W198.
54. Giurgiu, M., Reinhard, J., Brauner, B., Dunger-Kaltenbach, I., Fobo, G., Frishman, G., Montrone, C., and Ruepp, A. (2019). CORUM: the comprehensive resource of mammalian protein complexes—2019. Nucleic Acids Res. *47*, D559–D563.
55. Yu, G., Wang, L.-G., Han, Y., and He, Q.-Y. (2012). clusterProfiler: an R Package for comparing biological themes among gene clusters. OMICS: A J. Integr. Biol. *16*, 284–287.